Accepted Manuscript

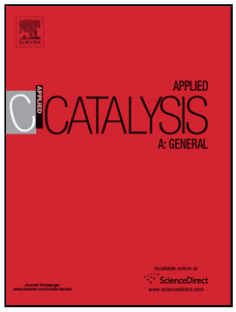

Title: Magnetic Crosslinked Copoly(ionic liquid) Nanohydrogel Supported Palladium Nanoparticles as Efficient Catalysts for the Selective Aerobic Oxidation of Alcohols

Authors: Mohammad Gholinejad, Mahmoud Afrasi, Nasser Nikfarjam, Carmen Nájera

PII: S0926-860X(18)30332-6
DOI: https://doi.org/10.1016/j.apcata.2018.07.009
Reference: APCATA 16735

To appear in: *Applied Catalysis A: General*

Received date: 23-3-2018
Revised date: 3-7-2018
Accepted date: 5-7-2018

Please cite this article as: Gholinejad M, Afrasi M, Nikfarjam N, Nájera C, Magnetic Crosslinked Copoly(ionic liquid) Nanohydrogel Supported Palladium Nanoparticles as Efficient Catalysts for the Selective Aerobic Oxidation of Alcohols, *Applied Catalysis A, General* (2018), https://doi.org/10.1016/j.apcata.2018.07.009

Magnetic Crosslinked Copoly(ionic liquid) Nanohydrogel Supported Palladium Nanoparticles as Efficient Catalysts for the Selective Aerobic Oxidation of Alcohols

Mohammad Gholinejad[ab], Mahmoud Afrasi[a], Nasser Nikfarjam[a]*, Carmen Nájera[c]*

[a] Department of Chemistry, Institute for Advanced Studies in Basic Sciences (IASBS), P. O. Box 45195-1159, Gavazang, Zanjan 45137-66731, Iran, E-mail: gholinejad@iasbs.ac.ir; nikfarjam@iasbs.ac.ir

[b]Research Center for Basic Sciences & Modern Technologies (RBST), Institute for Advanced Studies in Basic Sciences (IASBS), Zanjan 45137-66731, Iran

[c]Departamento de Química Orgánica and Centro de Innovación en Química Avanzada (ORFEO-CINQA), Universidad de Alicante, Apdo. 99, E-03080-Alicante, Spain.

Dedicated to Prof. Habib Firouzabadi on the occasion of his 75th birthday.

Graphical Abstract

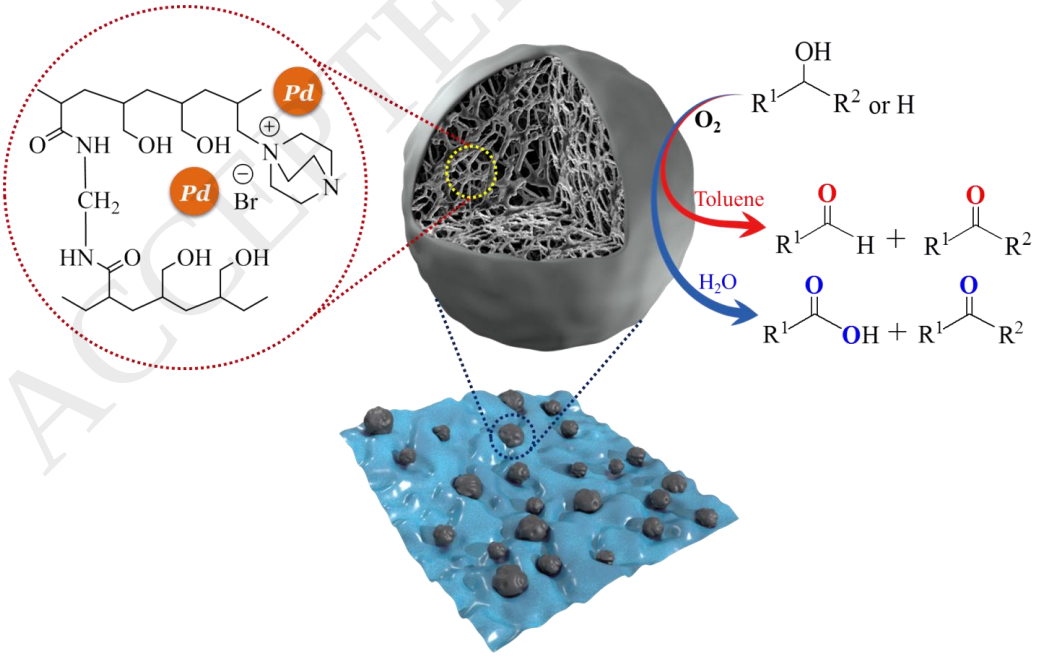

Research Highlights

- Novel magnetic nanohydrogel supported Pd NPs are synthesized and characterized.
- This material showed high efficiency for selective aerobic oxidation of alcohols.
- Catalyst was magnetically recovered and recycled for several times

Abstract:

Nowadays it is still a great sustainable processes challenge to produce efficient, selective and easy magnetic recovery and recycling catalysts for oxidation of alcohols using air as the oxidant. In this work, a new magnetic nanohydrogel comprising [DABCO-allyl][Br] ionic liquid, allyl alcohol and *N*,*N*'-methylenebis(acrylamide) is used for stabilization of small and highly uniform palladium nanoparticles of 3-4 nm size MXCPILNHG@Pd. This material has been characterized by Fourier-transform infrared spectroscopy (FTIR), atomic adsorption spectroscopy (AAS), thermogravimetric analysis (TGA), transmission electron microscopy (TEM), scanning electron microscopy (SEM), energy dispersive spectroscopy (EDS), SEM-Map, energy-dispersive X-ray spectroscopy (EDX), X-ray photoelectron spectra (XPS), vibrating-sample magnetometer (VSM) and dynamic light scattering (DLS). According to optimization of cross-linking degree and ratio of DABCO-IL, MXCPILNHG-2@Pd is found as a highly selective catalyst in oxidations of primary alcohols to the corresponding aldehydes in toluene and to acids in water. Furthermore, secondary alcohols were reacted efficiently to the corresponding ketones in both toluene and water. Catalyst is magnetically recovered and recycled for several times in both toluene and water and the reused catalysts are characterized by TEM and XPS.

Keywords: Magnetic, Nanohydrogel, Palladium, Oxidation, Alcohols

1- Introduction

The oxidation of alcohols to carbonyl compounds is an essential transformation in synthetic organic chemistry because of obtained aldehydes and ketones are basic precursors for synthesis of many drugs, vitamins and fragrances[1–3]. In particular, the selective oxidation of primary alcohols to the corresponding aldehydes or acids has been widely approved as one of the most important transformations from current chemical industry [4–13]. In the past two decades, extensive attention has been paid to the use of transition metals as catalysts as a better alternative than the conventional waste-producing oxidation procedures which require stoichiometric amounts of toxic inorganic salts [4–28]. Among the different oxidizing agents, oxygen produces water as the only byproduct and therefore is highly desirable from economic and green chemistry standpoints. Different complexes and salts of transition metals, such as Fe [29], Ru [30], Co [31], Cu [32], and Au [33] have been employed for this useful reaction. However, in comparison with the other transition metals, palladium [34–40] is one of the best efficient catalyst for the aerobic oxidation of alcohols under homogeneous or heterogeneous reaction conditions [41–61]. Due to contaminants of toxic palladium with products and also high price of palladium catalysts, recently many heterogeneous palladium catalysts have been developed for oxidation reaction of alcohols [62–72]. However, in spite of the great achievements in this field, most of the heterogeneous catalysts are difficult to separate from the reaction mixture by standard laboratory methods such as filtration and centrifugation. One approach to solve this problem is the use of magnetic catalysts which can be easily separated from the reaction mixture by an external magnetic field and match with green and sustainable chemistry points of view. Along this line, iron oxide nanoparticles with large ratio of surface area to volume, superparamagnetic behavior and low toxicity are excellent supports for the stabilization of palladium nanoparticles in

different organic transformations [73–89]. However, to date, few magnetite nanoparticles supported palladium catalysts have been prepared and successfully used in the aerobic oxidation of alcohols.

Nowadays chemists are interested in using ionic liquids as green solvents, catalysts and reagents. Despite outstanding physicochemical properties of ionic liquids (ILs) as alternative reaction media, their widespread utilization as solvent or catalyst are limited by the following drawbacks[90]: a) consume of large amounts of ILs is relatively costly and may cause toxicological problems, b) ILs play a minor role in the catalyzed reactions due to their higher viscosity and c) difficulties in product separation and catalyst recovery because of ILs homogeneity. To cope with these drawbacks, the concept of supported ionic liquids has been developed to associate both advantages of ILs and heterogeneous support materials. Several efforts have been made to immobilize ILs onto the support materials such as mesoporous silica [91–93], silica gel [94–96], polymers [97–99] and magnetic nanoparticles [100–102]. Heterogenization of ILs onto the material used as support has some problems such as tedious and difficult procedures of ILs grafting onto the surface of the support and low thermal stability of grafted ILs. Also, the normal grafting of ILs onto the solid materials is offering only one available layer on solid surface for immobilization which in turn leads to the low loading amount of grafted ILs. Hence, the low loading of ILs causes to use a large amount of solid support materials which in turn results in consuming a large amount of organic solvents in catalysis reactions and difficulty in separation/recovery of the used catalysts. Consequently, the available multi-layer onto the solid material surface for IL immobilization was proposed as a good technique to enhance IL loading amount [103–107]. But to avoid several boring steps [108]

looking for a simple and facile way for applying multi-layer on the solid support materials seems required.

In the present work, we report the synthesis of a novel magnetically copoly(ionic liquid) network catalyst in the nanoscale sizes, so-called magnetic x-linked PIL nanohydrogel (MXCPILNHG). These particles are prepared through the crosslinking copolymerization of a monomer bearing IL via a miniemulsion polymerization method followed by the loading of palladium nanoparticles (Pd NPs) to the IL groups in the network. The efficiency of this catalyst has been applied to the selective aerobic oxidation of alcohols.

2. Experimental

2.1. General remarks.

All materials were purchased from Sigma-Aldrich, Acros and Merck Millipore. Reactions were monitored by gas chromatography Varian CP-3800. ^{1}H NMR and ^{13}C NMR spectra were recorded at 400 MHz and 100 MHz, respectively on a Bruker Avance HD apparatus in $CDCl_3$. Chemical shifts are given on the δ-scale in ppm, and residual solvent peaks were used as internal standards. X-ray diffraction (XRD) patterns were recorded using Philips X'Pert Pro instrument. The TEM and SEM mapping images were captured with EOL JEM-2010 and Hitachi S3000N. (XPS) analyses were performed using a K-Alpha spectrometer. The weight loss of samples was measured using a thermogravimetry (NETZSCH STA 409) under an N2 flow rate of 20 ml.min-1 with a heating rate of 10 °C·min-1 from 30 to 800 °C. The diluted aqueous suspension of MXCPILNHG-2 particles was set on a clean glass slide and then vacuum-coated with gold. Digital images of the samples were acquired with Hitachi S4160 FE-SEM operating at 20 kV. FT-IR study of samples were performed using FT-IR spectrophotometer (Bruker vector 22 spectrophotometer, Germany) by preparing their KBr pellets from 400 to 4000 cm^{-1}. Magnetic

measurements were performed using vibration sample magnetometry (VSM), (MDK Co. Kashan, Iran) analysis.

2.2. Preparation of Fe_3O_4 NPs.

$FeCl_3 \cdot 6\ H_2O$ (11.0 g) and $FeCl_2 \cdot 4H_2O$ (4.0 g) were dissolved in deionized water (250 mL) and the mixture was stirred using a mechanical stirrer under an argon atmosphere. To the resulting mixture, aqueous ammonia (25 %, 40 mL) was added slowly over 20 min, and the mixture was stirred at 80 $^{\circ}$C for 4 h. A black precipitate of Fe_3O_4 was collected by using an external magnet and washed with deionized water (3 × 20 mL) and ethanol (3 × 20 mL) and finally dried under vacuum.

2.3. Preparation of Fe_3O_4@SiO_2.

To the 30 min sonicated Fe_3O_4 NPs (1 g) in ethanol (200 mL), tetraethyl orthosilicate (2 mL) and aqueous ammonia (25 %, 6 mL) were added and the resulting mixture was stirred for 24 h at room temperature. Fe_3O_4@SiO_2 NPs were separated by an external magnet and washed with EtOH (3×10 mL) dried in oven at 60 °C.

2.4. Synthesis of [DABCO-Allyl] [Br].

To a flask containing a solution of DABCO (24 mmol, 2.69 g) in ethyl acetate (50 mL), allyl bromide (20 mmol, 1.73 mL) was added and the resulting mixture was stirred for 24 h at room temperature. Then, the obtained solid was crystalized in diethyl ether and dried in oven at 50 °C. NMRs characterization verified the successful synthesis of [DABCO-Allyl][Br] (Figures S1 and S2). ^{1}H NMR: δ 5.97-5.87 (m, 1H), 5.67-5.58 (m, 2H), 3.84 (d, 2H, *J=8*), 3.35 (t, 6H), 3.12 (t, 6H). ^{13}C NMR: δ 129.07, 123.60, 66.41, 52.00, 44.42.

2.5. Preparation of Fe_3O_4@SiO_2@vinyl.

Fe_3O_4@SiO_2 (1 g) was sonicated in dry toluene (30 mL) for 30 min, and then dichloromethylvinylsilane (4 mmol, 0.52 mL) was added under inert conditions. The resulting mixture was stirred for 24 h at 80 °C under argon protection. Then, the reaction mixture was subjected to magnetic separation and the solid was separated giving Fe_3O_4@SiO_2@vinyl which was washed with EtOH (3×10 mL) and dried in an oven at 60 °C.

2.6. Preparation of MXCPILNHG-2.

These nanohydrogels were prepared via an inverse miniemulsion polymerization method. Fe_3O_4@SiO_2@vinyl (0.43 g), [DABCO-Allyl][Br] (2.15 mmol, 0.5 g), allyl alcohol (50 mmol, 3.4 mL) and *N*,*N*'-methylenebis(acrylamide) as crosslinker (4.34 mmol, 0.67 g) were dispersed in water (4.8 mL) with the aid of mechanical stirrer to form the water phase. Benzoyl peroxide as radical initiator (0.11 g) and Span80 as surfactant (1.19 g) were dissolved in cyclohexane (38.5 mL) to form the oil phase. Then, the water phase was added to the oil phase under vigorous mechanical stirring at room temperature for 1 h. The resulted inverse emulsion was miniemulsified using sonication (at amplitude of 50% in pulse mode) for 10 min in an ice-water bath to avoid unwanted polymerization. The obtained stable miniemulsion was quickly transferred to a three-necked round-bottomed flask equipped with a condenser, argon inlet and mechanical stirrer in the oil bath and was purged with argon. Finally, polymerization occurred at 70 °C under constant stirring of 500 rpm. After 24 h, the mixture was cooled by leaving it at room temperature for 1 h. The resulting nanoparticles were separated using an external magnet and washed several times by cyclohexane and water to remove impurities and unreacted monomers. The particles were dried in the oven at 50 °C for 12 h and then in a vacuum oven at 50 °C for another 12 h.

2.7. Synthesis of MXCPILNHG-2 supported palladium NPs catalyst.

MXCPILNHG-2 (500 mg) was sonicated in water (10 mL) for 15 min. Then, a solution of Na_2PdCl_4 (0.047 mmol, 14 mg) in H_2O (5 mL) was added slowly and the mixture was stirred for 1 h at room temperature. Then, a solution of $NaBH_4$ (0.8 mmol, 30 mg in 5 mL H_2O) was added during the 15 min and mixture was stirred for 24 h at room temperature under argon atmosphere. The resulting solid was separated magnetically, washed with water (3 × 20 mL) and ethanol (3 × 20 mL), and dried in an oven at 60 ^{o}C. The loading of Pd on the obtained material was determined by atomic adsorption spectroscopy analysis to be 0.1 mmol·g^{-1}.

2.8. General procedure for the oxidation of alcohol to aldehyde and acid (or ketone):

In a 5 mL glass flask, catalyst (10 mg, containing 0.2 mol% Pd), alcohol (0.5 mmol), K_2CO_3 (104 mg, 0.75 mmol) and H_2O or toluene (2 mL) were added and reaction mixture was stirred continuously at 90 ^{o}C for the desired time under O_2 atmosphere (from a balloon). Then, in the case of water as solvent, products were extracted with ethyl acetate and the catalyst was recovered by an external magnet. Yields of desired products were determined by gas chromatography.

2.9. Contact angle measurement for series of MXCPILNHG@Pd:

Compact pellets of all the prepared nanoparticles (both crosslink and DABCO-IL series) were prepared using stainless steel die-set and hydraulic press. Fine powder of nanoparticles was pressed for 5 minutes to form smooth pellets, 7 mm in diameter. The contact angle was determined with deionized water, using camera (Canon 70D) and ImageJ2x software. Three readings were taken in order to obtain an average over the heterogeneity of the surfaces. The pellets were placed in a vacuum oven at 50 °C for 12 h before measurements.

3. Results and discussion

3.1. Materials and characterization

The preparation steps for the magnetic hydrogel supported palladium NPs are presented in Scheme 1. Fe_3O_4 NPs were prepared from the reaction of $FeCl_3 \cdot 6H_2O$ and $FeCl_2 \cdot 4H_2O$ using a simple co-perception method. Core/shell Fe_3O_4@SiO_2 NPs were obtained from the reaction of Fe_3O_4 NPs and tetraethyl orthosilicate via a sol–gel process. TEM images showed thickness of SiO_2 shell to be around 4 nm (Figure S3), and also the results of porosimetry revealed the BET surface area of 37 $m^2 \cdot g^{-1}$ for Fe_3O_4@SiO_2. Carbon-carbon double bound was introduced on core/shell surface via the reaction of dichloro(methyl)vinylsilane with Fe_3O_4@SiO_2 NPs. Then, Fe_3O_4@SiO_2@vinyl was allowed to undergo polymerization with the already prepared [DABCO-allyl] [Br] salt, allyl alcohol and *N*,*N'*-methylenebis(acrylamide) as crosslinking agent in a mixture of cyclohexane/water and Span 80 (sorbitan oleate) as nonionic surfactant in the presence of benzoyl peroxide as an initiator. Final nanomagnetic hydrogel supported Pd NPs were obtained via the reaction of polymer modified Fe_3O_4 NPs with Na_2PdCl_4 and $NaBH_4$ under argon. The loading of Pd on the obtained solid was determined by atomic absorption spectroscopy analysis to be 0.1 mmol/g. The obtained magnetic composite is referred as MXCPILNHG@Pd NPs through the text of this article.

The surfaces of prepared magnetic compounds were investigated by FT-IR spectroscopy (Figure 1). In the case of the FT-IR spectrum of Fe_3O_4@SiO_2 peaks at 1097 and 1637 cm^{-1} related to the Si–O–Fe and bending vibration of the adsorbed water on the surface, respectively, were observed (Figure 1A). Besides, a new peak was observed at 1642 cm^{-1} related to C=C stretching for Fe_3O_4@SiO_2@vinyl (Figure 1B). The characteristic peaks for the MXCPILNHG-2 occurs at 3300-3600 cm^{-1} for the O-H stretching of allyl alcohol, 2928 and 2855 for the C-H stretching of

methylene and methine groups in the backbone of polymer. In addition, peaks at 3064, 1453, 1655 and 1532 cm^{-1} were attributed the N-H, C-N, free C=O and H-bonded C=O stretching of amide, respectively (Figure 1A).

Thermogravimetric analysis (TGA) was performed to study of the thermal properties of Fe_3O_4@SiO_2@vinyl and MXCPILNHG-2 (Figure 2). The TGA thermogram for Fe_3O_4@SiO_2@vinyl showed two main weight losses between 25-800 °C (Figure 1). The first weight loss was attributed to water and or physically adsorbed solvents and the second one is related to the successful grafting of vinyl groups on the surface of the core-shell magnetic nanoparticles (Figure 2A, S13). While, the TGA thermogram of the final nanohydrogel displayed three-step weight-loss profiles which of that the first one was attributed to the water and or physically adsorbed solvents (Figure 2B, S14). Dequaternization of the ammonium generally happens in the thermal degradation of ammonium containing polymers and the mechanism of this phenomenon occurs through two main suggested pathways; nucleophilic substitution and Hofmann elimination [109–111]. Therefore, one can conclude that the second weight loss is related to the dequaternization of DABCO mainly followed a reverse nucleophilic substitution mechanism (Scheme S1). These results are consistent with the finding of Zhang et al. where they studied the thermal degradation of copolymers based on N-4-vinylbenzyl-N'-alkyl DABCO BrCl (VBDCxBrCl) and *n*-butyl acrylate. They reported the 5 wt.% loss temperature values (T_d) of DABCO salt-containing copolymers ranged from 190 to 290 °C when ionic monomer varied from 42 to 1 mol % [111]. Whereas, the measured T_d value for MXCPILNHG-2 with 3.95 mol % of DABCO-IL monomer was around 245 °C, indicating the degradation mechanism for our case follows through a nucleophilic substitution mechanism, but it needs to be studied in more details. And finally, the third weight-loss step corresponded to the polymer backbone degradation,

mainly poly(allylalcohol) with initiation and maximum degradation temperatures of around 345.7 and 474 .8 °C, respectively [112]. The residue of around 31 wt. % is also attributed to the content of core-shell magnetic nanoparticles.

Magnetization curves for Fe_3O_4 NPs, Fe_3O_4NPs@SiO_2@vinyl, and magnetic hydrogel supported palladium were also studied (Figure 3). Results indicate a major decrease in the magnetization value of Fe_3O_4NPs@SiO_2@vinyl with respect to Fe_3O_4 NPs confirming the successful introduction of silyl and double bond shell. Also, a decrease in the magnetization value of magnetic hydrogel supported palladium is due to the effective polymerization around Fe_3O_4NPs@SiO_2@vinyl nanoparticles. However, in all samples Zero coercivity and remanence on the magnetization loop was observed without the presence of hysteresis loop, suggesting the superparamagnetic nature of the samples (Figure S15).

The field emission scanning electron microscopy (FE-SEM) micrographs revealed a paste-like morphology for MXCPILNHG-2 particles in the dried form (Figure 4). The size distribution of particle was obtained by manually measuring of at least 400 particles using JMicrovision 1.2.7 software. Then, the data was fitted by Gaussian function and the average particles size was calculated by the following equation: $\bar{D} = \sum d_i n_i / \sum n_i$, where n_i is the number of particles with diameter d_i. The average size of around 182 nm was found for these nanoparticles. While, dynamic light scattering (DLS) analysis revealed a hydrodynamic diameter of around 203nm for these particles (Figure S4). This difference can be attributed to the swelling capability of the particles in aqueous media, i.e. hydrogelic properties.

Transmission electron microscopy (TEM) images of final nanohydrogels showed the presence of polymer sheets around magnetic nanoparticles. TEM images also indicate incorporation of uniformly dispersed Pd NPs with the calculated average size of 3.5 nm (Figure 5). Also, scanning tunneling microscopy (STM) images of MXCPILNHG-2@Pd showed the presence of the Pd NPs (bright dots) on the surface of the final hydrogel structure (Figure S5). As well, BET isotherm of MXCPILNHG-2 before and after loading of Pd NPs showed no obvious difference in curves, indicating no obvious changes in structure (Figure S6-A). The degree of hysteresis loop, the gap between adsorption curve and desorption curve, in the isotherm of final hydrogel particle increased with increasing of Pd content (from 0.05 to 0.3 mmol of Pd, see Table S5 and Figure S6-B) and this is mainly due to capillary condensation effect. In other word the observed pressure difference between gas adsorption and desorption is probably because of locating of Pd nanoparticles inside pores in final hydrogel structure (bottle-neck structure) and this effect is intensified with increasing of Pd nanoparticle (Figure S6-B). Moreover, BET measurements showed that the surface area of MXCPILNHG-2 (25 $m^2.g^{-1}$) was increased by addition of Pd NPs (28 $m^2.g^{-1}$), maybe due to the added surface area by Pd NPs (Table S5). Consequently, one concluded that Pd NPs were located both inside and surface of the final hydrogel structure.

X-ray diffraction (XRD) analysis of prepared magnetic hydrogel showed related Bragg's reflections to the Fe_3O_4 NPs in 2Θ = 30.2, 35.5, 43.4, 53.5, 57.2, and 62.8° correspond to the (210), (311), (400), (422), (511), and (440) planes, respectively. In addition, these results showed Bragg's reflections related to palladium in 2Θ = 40.1, 46.8, and 68.2° and also related to silica shells in 2Θ = 22° (Figure 6) [113].

The X-ray photoelectron spectrum (XPS) of MXCPILNHG-2@Pd was also studied. XPS study of Fe 2p region shows two main binding energy peaks area (deconvoluted by six peaks) related

to 2p3/2 and Fe 2p1/2. Peaks centered at 712.7, 726.2 eV are related to Fe(III) oxidation state Furthermore the satellites at 719.1 eV and 732.9 eV are related to Fe^{3+} in the Fe_2O_3 phase, suggesting that the surface of Fe_3O_4 was partially oxidized to γ-Fe_2O_3. Also peaks at 710.5 and 724.3 eV are good agreement with Fe(II) and in the Fe_3O_4 structure [114,115] (Figure 7A). The XPS spectra in C 1s region showed three peaks centered at 284.7 and 286.9 and 288.5 eV, which are related to C-C or C=C, C-N or C-O and C=O forms of carbon, respectively [116,117] (Figure 7B). XPS study in Pd 3d region showed the presence of two intensive doublets at 335.5 and 340.7 eV related to Pd(0) and peaks at 337 and 342.5 eV related to Pd(II) species (Figure 7C). Results indicated that 74.9 % of palladium is in metallic Pd(0) form [118]. Also, the N1s core level spectrum shows a main peak at 399.6 eV, which is attributable to the neutral amine and a minor peak at 402 eV, which is related to positively charged quaternary nitrogen species [119] (Figure 7D).

Furthermore, energy dispersive spectroscopy (EDS) confirmed presence of different elements such as Pd, N, Si, Fe, and C were in the structure of magnetic hydrogel supported Pd NPs (Figure 8). On the other hand, SEM-Map images showed the presence of C, N and Pd in highly uniformly in magnetic hydrogel structure (Figures S7 and S8).

3.2.Catalytic performance

Catalytic activity of final Pd loaded magnetic nanohydrogels MXCPILNHG-2@Pd was examined in the aerobic oxidation of alcohols. Initially, selective aerobic oxidation of benzyl alcohol in toluene or H_2O solvents and K_2CO_3 as the base at 90 °C was selected as benchmark reaction. In order to find nanoparticles with high catalyst efficiency as well as high selectivity ability, two series of nanoparticles were synthesized. The first series, MXCPILNHG-crosslink, which of that the mole percent of the methylene bisacrylamide (MBA, as crosslinker) to the total

content of two monomers was increased from 4.5 to 8.3 and 15.0 %, named MXCPILNHG-1, MXCPILNHG-2 and MXCPILNHG-3, respectively (Table S1). In this series, it was curious to find the effect of hydrogel pore size, induced by crosslinking degree, on the catalyst activity and selectivity of nanoparticles and in the second series (i.e., MXCPILNHG-DABCO-IL), the mole percent of DABCO-IL to the total content of monomers was decreased from 12.4 to 4.1 and 2.2 % (named MXCPILNHG-4, MXCPILNHG-2, MXCPILNHG-5) in order to answering the following question; how the hydrophobicity of nanoparticles affects to catalyst efficiency and selectivity (Table S2).

In the MXCPILNHG-crosslink series, increasing of the crosslinking degree leads to a decrease in pore size of the obtained nanohydrogel. Therefore, it is expected that the confined pores in the higher crosslinking degree can limit the reagent transportation inside the nanohydrogel.

Nevertheless, the yields of the obtained products (benzaldehyde and benzoic acid) in the related solvents were decreased for MXCPILNHG-3 due to the mentioned compact structure of nanoparticle (Table S3). Also, the results revealed that the acid product yield was not actually varied with increasing of crosslinking degree for MXCPILNHG-1 and MXCPILNHG-2 (Table S3). But for these two catalysts, the aldehyde product yield was increased from 5 to 98 % in toluene as solvent. It seems that the benzyl alcohol has more tendency toward inside of particles in MXCPILNHG-2 than in MXCPILNHG-1 being oxidized to aldehyde in toluene as solvent. This tendency may be related to the hydrophobization effect of the crosslinking process, because for every linkage, one methylene group and two amide groups (with low capability of H-bond forming due to the strong resonance) are replaced by two hydroxyl groups. To confirm this claim, we checked their wettability by measuring contact angle of the particles. The results

showed that contact angle was increased with crosslinking degree; compare 53, 63 and 74° for MXCPILNHG-1, MXCPILNHG-2 and MXCPILNHG-3, respectively (Figure S9).

In the next step, we were looking for the optimized content of DABCO-IL in MXCPILNHG-DABCO-IL series. In the lowest content of DABCO-IL, i.e. MXCPILNHG-5, the yield of both products was decreased (Table S4).

This reduction in yielding can be related to the low loading of Pd NPs induced by the low content of DABCO-IL in the nanoparticle. And, the comparison between MXCPILNHG-4 and MXCPILNHG-2 revealed that the acid product yield was not actually changed, but the aldehyde product yield was decreased for the sample with the higher content of DABCO-IL, i.e. MXCPILNHG-4 (Table S4). The reason may lie in the fact of hydrophilization effect of DABCO-IL monomer containing two hydration sites, namely quarter ammonium. Accordingly, the tendency of nanoparticles for dispersion in toluene for MXCPILNHG-4 is lower than MXCPILNHG-2 and the catalyst efficiency for aldehyde product was declined from 98 to 10% (Table S4). For further proof, contact angle of particles was measured and its value was increased with lowering of the DABCO-IL content; compare 54, 63 and 80° for MXCPILNHG-4, MXCPILNHG-2 and MXCPILNHG-5 (Figure S9).

Based on the observed data from Tables S3 and S4, it seems that the MXCPILNHG-2 in both series has the best catalyst efficiency and selectivity and therefore, MXCPILNHG-2 was chosen as optimized formulation for further studies. To insure that toluene and water are best solvents for selective oxidation of benzyl alcohol to benzaldehyde and benzoic acid, respectively, the effect of other solvents such as 1,4-dioxane, CH_3CN, and DMA in the presence of 0.2 mol% of MXCPILNHG-2@Pd were studied (Table 1, entries 1-3). Results indicated formation of low yields for the desired oxidation products. Using other bases such as NaOAc, *t*-BuOK and base-

free reaction conditions gave low conversion in both toluene and H_2O (Table 1, entries 4-9). In addition, lowering the Pd loading, reaction times and temperature afforded low reaction conversion in both toluene and H_2O as solvents (Table 1, entries 10-15). It should be noted that using Fe_3O_4@SiO_2@Pd as catalyst reactions gave very low yields and starting material was intact (Table 1, entries 16-17).

Having the optimized reaction conditions in hand, aerobic oxidation of different primary alcohols was studied. Reactions of benzylic alcohols having electron-donating and electron-withdrawing groups as well as 1-naphthylmethanol in H_2O and toluene proceed efficiently and selectively acid and aldehydes were obtained (Table 2, entries 1-10). Reaction of 2-furanylmethanol as the heterocyclic primary alcohol was also studied. It is worth noting that 2-furanylmethanol is unstable alcohol in water and produce undesirable polymeric products. However, result of reaction in toluene showed highly selective formation of furfural in 96 % yield (Table 2, entry 11). Also, oxidation of 1-octanol as an aliphatic alcohol proceeded very well and products were obtained selectively in excellent yields (Table 2, entry 12). Reaction of cinnamyl alcohol as allylic alcohol in water gave moderate conversion with excellent selectivity to cinnamaldehyde while its reaction in toluene gave excellent conversion and selectivity to cinnamic acid (Table 2, entry 13).

We have also studied the oxidation of secondary alcohol under the optimized reaction conditions. Results of our study indicated that 1-phenylethanol, 1-phenylpropan-1-ol, 1,2,3,4-tetrahydronaphthalen-1-ol, benzhydrol, and 4-*tert*-butylcyclohexanol were performed very well in both toluene and water and the corresponding ketones were obtained in high to excellent yields (Table 3, entries 1-5). Reaction of cyclooctanol in water proceed well and cyclooctanone

was obtained in 88 % yield. However, the reaction in toluene was sluggish and low yield for corresponding ketone was obtained (Table 3, entry 6).

Catalytic activity and TOF of MXCPILNHG-2@Pd is compared with some of the reported catalysts in oxidation of benzyl alcohol as a common substrate (Table 4). In spite of high activity of some reported catalysts, results indicated overall activity of MXCPILNHG-2.

3.3. Recycling of the catalyst

Finally, recycling of the catalyst was studied for the oxidation reaction of benzyl alcohol under the optimized reaction conditions. For this purpose, after completion of reaction, catalyst was easily separated by external magnet and after washing with ethyl acetate was reused in another batch (Figure S15). Results indicated that the catalyst was recyclable up to 5 consecutive runs with small decrease in activity (Figure 9). However, yield was dropped to 68 and 74 % in ran 6 and to 35 and 43 % in run 7 in toluene and water respectively. Measurement of Pd content in each cycle indicated that dropping of yields are match with ratio of Pd leaching during the recycling (Table S6).

3.4.1. Characterization of reused catalyst

TEM images of reused catalysts in both toluene (Figure 10A-C) and water (Figure 10D-F) in different magnification indicated preservation of the catalyst structure and the presence of partially aggregate Pd NPs in bigger size ($\overline{D}$ = 7.4 nm for toluene and $\overline{D}$ = 9.3 nm for H_2O) with respect to the Pd NPs in the fresh catalyst ($\overline{D}$ = 3.5 nm).

XPS study of the reused catalyst after 5 runs in Pd 3d region showed different content of Pd (II) and Pd(0) species in water and toluene (Figure 11). While ratio of Pd(0)/Pd(II) was very similar to fresh catalyst, results for reused catalyst in water showed noticeable increasing of Pd(II) form with respect to the fresh catalyst. This may due to the good diffusion of oxygen in H_2O with respect to toluene.

Conclusion

The new catalyst based on the palladium loaded magnetic nanohydrogel bearing ionic liquid sites (MXCPILNHG@Pd) can be prepared and characterized by different techniques. By optimization of crosslinking degree and DABCO-IL content, MXCPILNHG-2@Pd with 8.3 % mol crosslinker and 4.1 % mol DABCO-IL showed good activity and selectivity toward oxidation of primary alcohols to aldehydes and acids in toluene and water respectively. In the case of secondary alcohols, the catalyst showed also high efficiency in both water and toluene. This catalyst can be easily recovered by separation with a magnet and reused for at least five cycles without detriment to its catalytic activity. Structure of reused catalyst in both toluene and water was studied by various techniques such as TEM and XPS.

Acknowledgements

The authors are grateful to Institute for Advanced Studies in Basic Sciences (IASBS) Research Council, Zanjan University and Iran National Science Foundation (INSF-Grant number of 95844587) for support of this work. The authors are also thankful to the Spanish Ministerio de Economía, Industria y Competitividad, Agencia Estatal de Investigación (AEI) and Fondo Europeo de Desarrollo Regional (FEDER, EU) (projects CTQ2016-76782-P and CTQ2016-

81797-REDC), the Generalitat Valenciana (PROMETEOII/ 2014/017) and the University of Alicante.

References

[1] P.T. Anastas, L.B. Bartlett, M.M. Kirchhoff, T.C. Williamson, M. Hudlicky, Oxidations in organic chemistry, Catal. Today. 55 (1990) 11–22.

[2] P.T. Anastas, L.B. Bartlett, M.M. Kirchhoff, T.C. Williamson, The role of catalysis in the design, development, and implementation of green chemistry, Catal. Today. 55 (2000) 11–22.

[3] A.M. Thayer, Catalyst suppliers face changing industry, Chem. Eng. News. 70 (1992) 27.

[4] D.-F. Yu, P. Xing, B. Jiang, N-Heterocyclic carbene-catalyzed aerobic oxidation of aryl alkyl alcohols to carboxylic acids, Tetrahedron. 25 (2015) 4269–4273.

[5] M.S. Ahmed, D.S. Mannel, T.W. Root, S.S. Stahl, Aerobic Oxidation of Diverse Primary Alcohols to Carboxylic Acids with a Heterogeneous Pd–Bi–Te/C (PBT/C) Catalyst, Org. Process Res. Dev. 21 (2017) 1388–1393.

[6] B. Karimi, M. Khorasani, H. Vali, C. Vargas, R. Luque, Palladium nanoparticles supported in the nanospaces of imidazolium-based bifunctional PMOs: The role of plugs in selectivity changeover in aerobic oxidation of alcohols, ACS Catal. 5 (2015) 4189–4200.

[7] M. Sharma, B. Das, M. Sharma, B.K. Deka, Y.-B. Park, S.K. Bhargava, K.K. Bania, Pd/Cu-oxide nanoconjugate at zeolite-Y crystallite crafting the mesoporous channels for selective oxidation of benzyl-alcohols, ACS Appl. Mater. Interfaces. 9 (2017) 35453–35462.

[8] L. Tang, X. Guo, Y. Li, S. Zhang, Z. Zha, Z. Wang, Pt, Pd and Au nanoparticles supported

on a DNA–MMT hybrid: efficient catalysts for highly selective oxidation of primary alcohols to aldehydes, acids and esters, Chem. Commun. 49 (2013) 5213–5215.

[9] C. Deraedt, D. Wang, L. Salmon, L. Etienne, C. Labrugère, J. Ruiz, D. Astruc, Robust, efficient, and recyclable catalysts from the impregnation of preformed dendrimers containing palladium nanoparticles on a magnetic support, ChemCatChem. 7 (2015) 303–308.

[10] L. Lei, Z. Wu, R. Wang, Z. Qin, C. Chen, Y. Liu, G. Wang, W. Fan, J. Wang, Controllable decoration of palladium sub-nanoclusters on reduced graphene oxide with superior catalytic performance in selective oxidation of alcohols, Catal. Sci. Technol. 7 (2017) 5650–5661.

[11] G. Chen, S. Wu, H. Liu, H. Jiang, Y. Li, Palladium supported on an acidic metal–organic framework as an efficient catalyst in selective aerobic oxidation of alcohols, Green Chem. 15 (2013) 230–235.

[12] J. Xu, J.-K. Shang, Y. Chen, Y. Wang, Y.-X. Li, Palladium nanoparticles supported on mesoporous carbon nitride for efficiently selective oxidation of benzyl alcohol with molecular oxygen, Appl. Catal. A Gen. 542 (2017) 380–388.

[13] S. Guadix-Montero, H. Alshammari, R. Dalebout, E. Nowicka, D.J. Morgan, G. Shaw, Q. He, M. Sankar, Deactivation studies of bimetallic AuPd nanoparticles supported on MgO during selective aerobic oxidation of alcohols, Appl. Catal. A Gen. 546 (2017) 58–66.

[14] A.J. Mancuso, D. Swern, Activated dimethyl sulfoxide: useful reagents for synthesis, Synthesis (Stuttg). 1981 (1981) 165–185.

[15] D.B. Dess, J.C. Martin, Readily accessible 12-I-5 oxidant for the conversion of primary and secondary alcohols to aldehydes and ketones, J. Org. Chem. 48 (1983) 4155–4156.

[16] B.A. Steinhoff, S.R. Fix, S.S. Stahl, Mechanistic study of alcohol oxidation by the Pd (OAc) 2/O2/DMSO catalyst system and implications for the development of improved aerobic oxidation catalysts, J. Am. Chem. Soc. 124 (2002) 766–767.

[17] R.D. Richardson, T. Wirth, Hypervalent iodine goes catalytic, Angew. Chemie Int. Ed. 45 (2006) 4402–4404.

[18] M. Uyanik, K. Ishihara, Hypervalent iodine-mediated oxidation of alcohols, Chem. Commun. (2009) 2086–2099.

[19] M. Uyanik, M. Akakura, K. Ishihara, 2-Iodoxybenzenesulfonic acid as an extremely active catalyst for the selective oxidation of alcohols to aldehydes, ketones, carboxylic acids, and enones with oxone, J. Am. Chem. Soc. 131 (2008) 251–262.

[20] D.G. Lee, U.A. Spitzer, Aqueous dichromate oxidation of primary alcohols, J. Org. Chem. 35 (1970) 3589–3590.

[21] F.M. Menger, C. Lee, Synthetically useful oxidations at solid sodium permanganate surfaces, Tetrahedron Lett. 22 (1981) 1655–1656.

[22] C. Parmeggiani, C. Matassini, F. Cardona, A step forward towards sustainable aerobic alcohol oxidation: new and revised catalysts based on transition metals on solid supports, Green Chem. 19 (2017) 2030–2050.

[23] C. Parmeggiani, F. Cardona, Transition metal based catalysts in the aerobic oxidation of alcohols, Green Chem. 14 (2012) 547–564.

[24] C.P. Vinod, K. Wilson, A.F. Lee, Recent advances in the heterogeneously catalysed aerobic selective oxidation of alcohols, J. Chem. Technol. Biotechnol. 86 (2011) 161–171.

[25] M.J. Schultz, M.S. Sigman, Recent advances in homogeneous transition metal-catalyzed aerobic alcohol oxidations, Tetrahedron. 62 (2006) 8227–8241.

[26] B.-Z. Zhan, A. Thompson, Recent developments in the aerobic oxidation of alcohols, Tetrahedron. 60 (2004) 2917–2935.

[27] O. Das, T.K. Paine, Aerobic oxidation of primary alcohols catalyzed by copper complexes of 1, 10-phenanthroline-derived ligands, Dalt. Trans. 41 (2012) 11476–11481.

[28] A. Mondal, A. Das, B. Adhikary, D.K. Mukherjee, Palladium nanoparticles in ionic liquids: reusable catalysts for aerobic oxidation of alcohols, J. Nanoparticle Res. 16 (2014) 2366.

[29] K. Lagerblom, P. Wrigstedt, J. Keskiväli, A. Parviainen, T. Repo, Iron-Catalysed Selective Aerobic Oxidation of Alcohols to Carbonyl and Carboxylic Compounds, Chempluschem. 81 (2016) 1160–1165.

[30] V. V Costa, M.J. Jacinto, L.M. Rossi, R. Landers, E. V Gusevskaya, Aerobic oxidation of monoterpenic alcohols catalyzed by ruthenium hydroxide supported on silica-coated magnetic nanoparticles, J. Catal. 282 (2011) 209–214.

[31] B. Karimi, Z. Naderi, M. Khorasani, H.M. Mirzaei, H. Vali, Ultrasmall Platinum Nanoparticles Supported Inside the Nanospaces of Periodic Mesoporous Organosilica with an Imidazolium Network: An Efficient Catalyst for the Aerobic Oxidation of Unactivated Alcohols in Water, ChemCatChem. 8 (2016) 906–910.

[32] B.L. Ryland, S.S. Stahl, Practical aerobic oxidations of alcohols and amines with homogeneous copper/TEMPO and related catalyst systems, Angew. Chemie Int. Ed. 53 (2014) 8824–8838.

[33] H. Wang, Y. Shi, M. Haruta, J. Huang, Aerobic oxidation of benzyl alcohol in water catalyzed by gold nanoparticles supported on imidazole containing crosslinked polymer, Appl. Catal. A Gen. 536 (2017) 27–34.

[34] A. Vasseur, R. Membrat, D. Gatineau, A. Tenaglia, D. Nuel, L. Giordano, Secondary Phosphine Oxides as Multitalented Preligands En Route to the Chemoselective Palladium-Catalyzed Oxidation of Alcohols, ChemCatChem. 9 (2017) 728–732.

[35] K. Ando, J. Nakazawa, S. Hikichi, Synthesis, Characterization and Aerobic Alcohol Oxidation Catalysis of Palladium (II) Complexes with a Bis (imidazolyl) borate Ligand, Eur. J. Inorg. Chem. 2016 (2016) 2603–2608.

[36] N. Armenise, N. Tahiri, N.N.H.M. Eisink, M. Denis, M. Jäger, J.G. De Vries, M.D. Witte, A.J. Minnaard, Deuteration enhances catalyst lifetime in palladium-catalysed alcohol oxidation, Chem. Commun. 52 (2016) 2189–2191.

[37] L.M. Dornan, M.J. Muldoon, A highly efficient palladium (II)/polyoxometalate catalyst system for aerobic oxidation of alcohols, Catal. Sci. Technol. 5 (2015) 1428–1432.

[38] K. Karami, N.H. Naeini, V. Eigner, M. Dusek, J. Lipkowski, P. Hervés, H. Tavakol, Palladium complexes with 3-phenylpropylamine ligands: synthesis, structures, theoretical studies and application in the aerobic oxidation of alcohols as heterogeneous catalysts, RSC Adv. 5 (2015) 102424–102435.

[39] S. Gowrisankar, H. Neumann, D. Gördes, K. Thurow, H. Jiao, M. Beller, A Convenient and Selective Palladium-Catalyzed Aerobic Oxidation of Alcohols, Chem. Eur. J. 19 (2013) 15979–15984.

[40] B. Karimi, D. Elhamifar, J.H. Clark, A.J. Hunt, Palladium containing periodic mesoporous organosilica with imidazolium framework (Pd@ PMO-IL): an efficient and recyclable catalyst for the aerobic oxidation of alcohols, Org. Biomol. Chem. 9 (2011) 7420–7426.

[41] P. Sangtrirutnugul, T. Chaiprasert, W. Hunsiri, T. Jitjaroendee, P. Songkhum, K. Laohhasurayotin, T. Osotchan, V. Ervithayasuporn, Tunable Porosity of Cross-Linked-Polyhedral Oligomeric Silsesquioxane Supports for Palladium-Catalyzed Aerobic Alcohol Oxidation in Water, ACS Appl. Mater. Interfaces. 9 (2017) 12812–12822.

[42] N. Gogoi, P. Bordoloi, G. Borah, P.K. Gogoi, Synthesis of Palladium Nanoparticle by Bio-reduction Method and Its Effectiveness as Heterogeneous Catalyst Towards Selective Oxidation of Benzyl alcohols in Aqueous Media, Catal. Letters. 147 (2017) 539–546.

[43] H. Veisi, S. Hemmati, M. Qomi, Aerobic oxidation of benzyl alcohols through biosynthesized palladium nanoparticles mediated by Oak fruit bark extract as an efficient heterogeneous nanocatalyst, Tetrahedron Lett. 58 (2017) 4191–4196.

[44] S. Campisi, D. Ferri, A. Villa, W. Wang, D. Wang, O. Kröcher, L. Prati, Selectivity control in palladium-catalyzed alcohol oxidation through selective blocking of active sites, J. Phys. Chem. C. 120 (2016) 14027–14033.

[45] L. Chen, T. Feng, P. Wang, Z. Chen, R. Yan, B. Liao, Y. Xiang, A recoverable sandwich phosphorotungstate stabilized palladium (0) catalyst for aerobic oxidation of alcohols in water, Appl. Catal. A Gen. 523 (2016) 304–311.

[46] A. Savara, I. Rossetti, C.E. Chan-Thaw, L. Prati, A. Villa, Microkinetic Modeling of Benzyl Alcohol Oxidation on Carbon-Supported Palladium Nanoparticles, ChemCatChem. 8 (2016) 2482–2491.

[47] A. Benyounes, S. Louisia, R. Axet, Z. Mahfoud, M. Kacimi, P. Serp, Green alcohol oxidation on palladium catalysts supported on amphiphilic hybrid carbon nanotubes, Catal. Today. 249 (2015) 137–144.

[48] O.O. Fashedemi, H.A. Miller, A. Marchionni, F. Vizza, K.I. Ozoemena, Electro-oxidation of ethylene glycol and glycerol at palladium-decorated FeCo@ Fe core–shell nanocatalysts for alkaline direct alcohol fuel cells: functionalized MWCNT supports and impact on product selectivity, J. Mater. Chem. A. 3 (2015) 7145–7156.

[49] S. Ghosh, A.-L. Teillout, D. Floresyona, P. de Oliveira, A. Hagege, H. Remita, Conducting polymer-supported palladium nanoplates for applications in direct alcohol oxidation, Int. J. Hydrogen Energy. 40 (2015) 4951–4959.

[50] Y. Lu, H. Zhu, J. Liu, S. Yu, Palladium Nanoparticles Supported on Titanate Nanobelts for Solvent-Free Aerobic Oxidation of Alcohols, ChemCatChem. 7 (2015) 4131–4136.

[51] V. Pascanu, A. Bermejo Gómez, C. Ayats, A.E. Platero-Prats, F. Carson, J. Su, Q. Yao, M.A. Pericàs, X. Zou, B. Martín-Matute, Double-Supported Silica-Metal–Organic Framework Palladium Nanocatalyst for the Aerobic Oxidation of Alcohols under Batch and Continuous Flow Regimes, ACS Catal. 5 (2014) 472–479.

[52] M.M. Dell'Anna, M. Mali, P. Mastrorilli, P. Cotugno, A. Monopoli, Oxidation of benzyl alcohols to aldehydes and ketones under air in water using a polymer supported palladium catalyst, J. Mol. Catal. A Chem. 386 (2014) 114–119.

[53] D. Sahu, C. Sarmah, P. Das, A highly efficient and recyclable silica-supported palladium catalyst for alcohol oxidation reaction, Tetrahedron Lett. 55 (2014) 3422–3425.

[54] Y. Yan, Y. Chen, X. Jia, Y. Yang, Palladium nanoparticles supported on organosilane-functionalized carbon nanotube for solvent-free aerobic oxidation of benzyl alcohol, Appl. Catal. B Environ. 156 (2014) 385–397.

[55] Y. Zhou, Z. Xiang, D. Cao, C. Liu, Preparation and characterization of covalent organic polymer supported palladium catalysts for oxidation of CO and benzyl alcohol, Ind. Eng. Chem. Res. 53 (2014) 1359–1367.

[56] K. Karami, M. Ghasemi, N.H. Naeini, Palladium nanoparticles supported on polymer: An efficient and reusable heterogeneous catalyst for the Suzuki cross-coupling reactions and aerobic oxidation of alcohols, Catal. Commun. 38 (2013) 10–15.

[57] B. Qi, Y. Wang, L.-L. Lou, L. Huang, Y. Yang, S. Liu, Solvent-free aerobic oxidation of alcohols over palladium supported on MCM-41, J. Mol. Catal. A Chem. 370 (2013) 95–103.

[58] S. Verma, D. Tripathi, P. Gupta, R. Singh, G.M. Bahuguna, R.K. Chauhan, S. Saran, S.L. Jain, Highly dispersed palladium nanoparticles grafted onto nanocrystalline starch for the oxidation of alcohols using molecular oxygen as an oxidant, Dalt. Trans. 42 (2013) 11522–11527.

[59] G. Wu, X. Wang, N. Guan, L. Li, Palladium on graphene as efficient catalyst for solvent-free aerobic oxidation of aromatic alcohols: Role of graphene support, Appl. Catal. B Environ. 136 (2013) 177–185.

[60] B. Karimi, H. Behzadnia, M. Bostina, H. Vali, A Nano-Fibrillated Mesoporous Carbon as an Effective Support for Palladium Nanoparticles in the Aerobic Oxidation of Alcohols "on Pure Water," Chem. Eur. J. 18 (2012) 8634–8640.

[61] D.S. Mannel, M.S. Ahmed, T.W. Root, S.S. Stahl, Discovery of Multicomponent Heterogeneous Catalysts via Admixture Screening: PdBiTe Catalysts for Aerobic Oxidative Esterification of Primary Alcohols, J. Am. Chem. Soc. 139 (2017) 1690–1698.

[62] X. Sun, Y. Zheng, L. Sun, Q. Lin, H. Su, C. Qi, Immobilization of palladium (II) complexes on ethylenediamine functionalized core–shell magnetic nanoparticles: An efficient and recyclable catalyst for aerobic oxidation of alcohols and carbonylative Suzuki coupling reaction, Nano-Structures & Nano-Objects. 5 (2016) 7–14.

[63] F. Zamani, S.M. Hosseini, Palladium nanoparticles supported on Fe3O4/amino acid nanocomposite: Highly active magnetic catalyst for solvent-free aerobic oxidation of alcohols, Catal. Commun. 43 (2014) 164–168.

[64] V. Polshettiwar, R.S. Varma, Nanoparticle-supported and magnetically recoverable palladium (Pd) catalyst: a selective and sustainable oxidation protocol with high turnover number, Org. Biomol. Chem. 7 (2009) 37–40.

[65] R.B.N. Baig, M.N. Nadagouda, R.S. Varma, Carbon-coated magnetic palladium: applications in partial oxidation of alcohols and coupling reactions, Green Chem. 16 (2014) 4333–4338.

[66] L. Kong, C. Wang, F. Gong, W. Zhu, Y. Zhong, X. Ye, F. Li, Magnetic Core–Shell Nanostructured Palladium Catalysts for Green Oxidation of Benzyl Alcohol, Catal. Letters. 146 (2016) 1321–1330.

[67] L. Zhang, P. Li, J. Yang, M. Wang, L. Wang, Palladium Supported on Magnetic Core–Shell Nanoparticles: An Efficient and Reusable Catalyst for the Oxidation of Alcohols into Aldehydes and Ketones by Molecular Oxygen, Chempluschem. 79 (2014) 217–222.

[68] A. Ramazani, M. Khoobi, F. Sadri, R. Tarasi, A. Shafiee, H. Aghahosseini, S.W. Joo, Efficient and selective oxidation of alcohols in water employing palladium supported nanomagnetic Fe3O4@ hyperbranched polyethylenimine (Fe3O4@ HPEI. Pd) as a new organic–inorganic hybrid nanocatalyst, Appl. Organomet. Chem. 32 (2018).

[69] C. Antonetti, L. Toniolo, G. Cavinato, C. Forte, C. Ghignoli, R. Ishak, F. Cavani, A.M.R. Galletti, A hybrid polyketone–SiO2 support for palladium catalysts and their applications in cinnamaldehyde hydrogenation and in 1-phenylethanol oxidation, Appl. Catal. A Gen. 496 (2015) 40–50.

[70] S. Verma, D. Verma, A.K. Sinha, S.L. Jain, Palladium complex immobilized on graphene oxide–magnetic nanoparticle composites for ester synthesis by aerobic oxidative esterification of alcohols, Appl. Catal. A Gen. 489 (2015) 17–23.

[71] Z. Zhang, J. Zhen, B. Liu, K. Lv, K. Deng, Selective aerobic oxidation of the biomass-derived precursor 5-hydroxymethylfurfural to 2, 5-furandicarboxylic acid under mild conditions over a magnetic palladium nanocatalyst, Green Chem. 17 (2015) 1308–1317.

[72] N. Mei, B. Liu, J. Zheng, K. Lv, D. Tang, Z. Zhang, A novel magnetic palladium catalyst for the mild aerobic oxidation of 5-hydroxymethylfurfural into 2, 5-furandicarboxylic acid in water, Catal. Sci. Technol. 5 (2015) 3194–3202.

[73] B. Karimi, F. Mansouri, H.M. Mirzaei, ChemCatChem 2015, 7, 1736, Web Sci. Times Cited. 33 (n.d.).

[74] D. Wang, C. Deraedt, L. Salmon, C. Labrugère, L. Etienne, J. Ruiz, D. Astruc, A tris (triazolate) ligand for a highly active and magnetically recoverable palladium catalyst of selective alcohol oxidation using air at atmospheric pressure, Chem. Eur. J. 21 (2015) 6501–6510.

[75] T. Karimpour, E. Safaei, B. Karimi, Y. Lee, Iron (III) Amine Bis (phenolate) Complex Immobilized on Silica-Coated Magnetic Nanoparticles: A Highly Efficient Catalyst for the Oxidation of Alcohols and Sulfides, ChemCatChem. (n.d.).**DOI:** 10.1002/cctc.201701217

[76] P.B. Bhat, R. Rajarao, V. Sahajwalla, B.R. Bhat, Immobilized magnetic nano catalyst for oxidation of alcohol, J. Mol. Catal. A Chem. 409 (2015) 42–49.

[77] B. Eftekhari-Sis, M. Akbari, A. Akbari, M. Amini, Vanadium (V) and Tungsten (VI) Oxoperoxo-Complexes Anchored on Fe3O4 Magnetic Nanoparticles: Versatile and Efficient Catalysts for the Oxidation of Alcohols and Sulfides, Catal. Letters. 147 (2017) 2106–2115.

[78] C. Kamonsatikul, T. Khamnaen, P. Phiriyawirut, S. Charoenchaidet, E. Somsook, Synergistic activities of magnetic iron-oxide nanoparticles and stabilizing ligands containing ferrocene moieties in selective oxidation of benzyl alcohol, Catal. Commun. 26 (2012) 1–5.

[79] X. Dong, X. Zhang, P. Wu, Y. Zhang, B. Liu, H. Hu, G. Xue, Divanadium-Substituted Phosphotungstate Supported on Magnetic Mesoporous Silica Nanoparticles as Effective and Recyclable Catalysts for the Selective Oxidation of Alcohols, ChemCatChem. 8 (2016) 3680–3687.

[80] Q. Zhou, Z. Wan, X. Yuan, J. Luo, A new magnetic nanoparticle-supported Schiff base

complex of manganese: an efficient and recyclable catalyst for selective oxidation of alcohols, Appl. Organomet. Chem. 30 (2016) 215–220.

[81] H. Keypour, S.G. Saremi, H. Veisi, R. Azadbakht, Novel Schiff base Mn (III) and Co (II) complexes supported on Co nanoparticles: efficient and recyclable magnetic nanocatalysts for alcohol oxidation, RSC Adv. 6 (2016) 77020–77029.

[82] F. Sadri, A. Ramazani, A. Massoudi, M. Khoobi, R. Tarasi, A. Shafiee, V. Azizkhani, L. Dolatyari, S.W. Joo, Green oxidation of alcohols by using hydrogen peroxide in water in the presence of magnetic Fe3O4 nanoparticles as recoverable catalyst, Green Chem. Lett. Rev. 7 (2014) 257–264.

[83] Z. Zheng, J. Wang, M. Zhang, L. Xu, J. Ji, Magnetic polystyrene nanosphere immobilized TEMPO: a readily prepared, highly reactive and recyclable polymer catalyst in the selective oxidation of alcohols, ChemCatChem. 5 (2013) 307–312.

[84] J. Zhu, P. Wang, M. Lu, Synthesis of novel magnetic silica supported hybrid ionic liquid combining TEMPO and polyoxometalate and its application for selective oxidation of alcohols, RSC Adv. 2 (2012) 8265–8268.

[85] B. Karimi, E. Farhangi, A Highly Recyclable Magnetic Core-Shell Nanoparticle-Supported TEMPO catalyst for Efficient Metal-and Halogen-Free Aerobic Oxidation of Alcohols in Water, Chem. Eur. J. 17 (2011) 6056–6060.

[86] R.L. Oliveira, P.K. Kiyohara, L.M. Rossi, High performance magnetic separation of gold nanoparticles for catalytic oxidation of alcohols, Green Chem. 12 (2010) 144–149.

[87] M. Dehghan, A. Motaharinejad, M. Saadat, R. Ahdenov, M. Babazadeh, R. Hosseinzadeh-

Khanmiri, Novel approach to synthesizing polymer-functionalized Fe3O4/SiO2–NH2 via an ultrasound-assisted method for catalytic selective oxidation of alcohols to aldehydes and ketones in a DMSO/water mixture, RSC Adv. 5 (2015) 92335–92343.

[88] X. Yao, C. Bai, J. Chen, Y. Li, Efficient and selective green oxidation of alcohols by MOF-derived magnetic nanoparticles as a recoverable catalyst, RSC Adv. 6 (2016) 26921–26928.

[89] F. Zamani, S. Kianpour, B. Nekooei, Cr (III)-containing Fe3O4/mercaptopropanoic acid-poly (2-hydroxyethyl acrylate) nanocomposite: Highly active magnetic catalyst for direct hydroxylation of benzene, J. Appl. Polym. Sci. 131 (2014).

[90] D. Zhao, Y. Liao, Z. Zhang, Toxicity of ionic liquids, Clean–soil, Air, Water. 35 (2007) 42–48.

[91] R. Kore, R. Srivastava, Synthesis of triethoxysilane imidazolium based ionic liquids and their application in the preparation of mesoporous ZSM-5, Catal. Commun. 18 (2012) 11–15.

[92] P. Han, H. Zhang, X. Qiu, X. Ji, L. Gao, Palladium within ionic liquid functionalized mesoporous silica SBA-15 and its catalytic application in room-temperature Suzuki coupling reaction, J. Mol. Catal. A Chem. 295 (2008) 57–67.

[93] T. Yokoi, Y. Kubota, T. Tatsumi, Amino-functionalized mesoporous silica as base catalyst and adsorbent, Appl. Catal. A Gen. 421 (2012) 14–37.

[94] D.A. Kotadia, S.S. Soni, Silica gel supported–SO3H functionalised benzimidazolium based ionic liquid as a mild and effective catalyst for rapid synthesis of 1-amidoalkyl

naphthols, J. Mol. Catal. A Chem. 353 (2012) 44–49.

[95] F. Shi, Q. Zhang, D. Li, Y. Deng, Silica-Gel-Confined Ionic Liquids: A New Attempt for the Development of Supported Nanoliquid Catalysis, Chem. Eur. J. 11 (2005) 5279–5288.

[96] A. Chrobok, S. Baj, W. Pudło, A. Jarzębski, Supported hydrogensulfate ionic liquid catalysis in Baeyer–Villiger reaction, Appl. Catal. A Gen. 366 (2009) 22–28.

[97] W. Chen, Y. Zhang, L. Zhu, J. Lan, R. Xie, J. You, A concept of supported amino acid ionic liquids and their application in metal scavenging and heterogeneous catalysis, J. Am. Chem. Soc. 129 (2007) 13879–13886.

[98] A.L. Becker, N. Welsch, C. Schneider, M. Ballauff, Adsorption of RNase A on cationic polyelectrolyte brushes: a study by isothermal titration calorimetry, Biomacromolecules. 12 (2011) 3936–3944.

[99] J. Yang, L. Qiu, B. Liu, Y. Peng, F. Yan, S. Shang, Synthesis of polymeric ionic liquid microsphere/Pt nanoparticle hybrids for electrocatalytic oxidation of methanol and catalytic oxidation of benzyl alcohol, J. Polym. Sci. Part A Polym. Chem. 49 (2011) 4531–4538.

[100] Y. Zhang, Y. Zhao, C. Xia, Basic ionic liquids supported on hydroxyapatite-encapsulated γ-Fe2O3 nanocrystallites: An efficient magnetic and recyclable heterogeneous catalyst for aqueous Knoevenagel condensation, J. Mol. Catal. A Chem. 306 (2009) 107–112.

[101] Y. Zhang, C. Xia, Magnetic hydroxyapatite-encapsulated γ-Fe2O3 nanoparticles functionalized with basic ionic liquids for aqueous Knoevenagel condensation, Appl. Catal. A Gen. 366 (2009) 141–147.

[102] Y. Jiang, C. Guo, H. Xia, I. Mahmood, C. Liu, H. Liu, Magnetic nanoparticles supported ionic liquids for lipase immobilization: Enzyme activity in catalyzing esterification, J. Mol. Catal. B Enzym. 58 (2009) 103–109.

[103] F.M. Moghaddam, S.E. Ayati, S.H. Hosseini, A. Pourjavadi, Gold immobilized onto poly (ionic liquid) functionalized magnetic nanoparticles: a robust magnetically recoverable catalyst for the synthesis of propargylamine in water, RSC Adv. 5 (2015) 34502–34510.

[104] A. Pourjavadi, S.H. Hosseini, S.A. AghayeeMeibody, S.T. Hosseini, Poly (basic ionic liquid) coated magnetic nanoparticles: High-loaded supported basic ionic liquid catalyst, Comptes Rendus Chim. 16 (2013) 906–911.

[105] A. Pourjavadi, S.H. Hosseini, Z.S. Emami, Cross-linked basic nanogel; robust heterogeneous organocalayst, Chem. Eng. J. 232 (2013) 453–457.

[106] F.M. Moghaddam, S.E. Ayati, H.R. Firouzi, S.H. Hosseini, A. Pourjavadi, Gold nanoparticles anchored onto the magnetic poly (ionic-liquid) polymer as robust and recoverable catalyst for reduction of Nitroarenes, Appl. Organomet. Chem. 31 (2017).

[107] A. Pourjavadi, M. Tajbakhsh, M. Farhang, S.H. Hosseini, Copper-loaded polymeric magnetic nanocatalysts as retrievable and robust heterogeneous catalysts for click reactions, New J. Chem. 39 (2015) 4591–4600.

[108] A. Pourjavadi, S.H. Hosseini, M. Doulabi, S.M. Fakoorpoor, F. Seidi, Multi-layer functionalized poly (ionic liquid) coated magnetic nanoparticles: highly recoverable and magnetically separable Brønsted acid catalyst, ACS Catal. 2 (2012) 1259–1266.

[109] S.T. Hemp, M. Zhang, M.H. Allen, S. Cheng, R.B. Moore, T.E. Long, Comparing

ammonium and phosphonium polymerized ionic liquids: thermal analysis, conductivity, and morphology, Macromol. Chem. Phys. 214 (2013) 2099–2107.

[110] S.R. Williams, E.M. Borgerding, J.M. Layman, W. Wang, K.I. Winey, T.E. Long, Synthesis and characterization of well-defined 12, 12-ammonium ionenes: Evaluating mechanical properties as a function of molecular weight, Macromolecules. 41 (2008) 5216–5222.

[111] L. Quach, T. Otsu, Head-to-head vinyl polymers. VI. Preparation and characterization of head-to-head poly (allyl alcohol) and its esters, J. Polym. Sci. Part A Polym. Chem. 20 (1982) 2501–2511.

[112] K. Zhang, K.J. Drummey, N.G. Moon, W.D. Chiang, T.E. Long, Styrenic DABCO salt-containing monomers for the synthesis of novel charged polymers, Polym. Chem. 7 (2016) 3370–3374.

[113] M. Gholinejad, M. Seyedhamzeh, M. Razeghi, C. Najera, M. Kompany-Zareh, Iron oxide nanoparticles modified with carbon quantum nanodots for the stabilization of palladium nanoparticles: an efficient catalyst for the suzuki reaction in aqueous media under mild conditions, ChemCatChem. 8 (2016) 441–447.

[114] W. Wang, B. Tang, B. Ju, Z. Gao, J. Xiu, S. Zhang, Fe 3 O 4-functionalized graphene nanosheet embedded phase change material composites: efficient magnetic-and sunlight-driven energy conversion and storage, J. Mater. Chem. A. 5 (2017) 958–968.

[115] X. Wang, Y. Liu, H. Han, Y. Zhao, W. Ma, H. Sun, Polyaniline coated Fe 3 O 4 hollow nanospheres as anode materials for lithium ion batteries, Sustain. Energy Fuels. 1 (2017) 915–922.

[116] R. Böhme, D. Spemann, K. Zimmer, Surface characterization of backside-etched transparent dielectrics, Thin Solid Films. 453 (2004) 127–132.

[117] J. Wang, X. Zhang, Y. Zhang, A. Abas, X. Zhao, Z. Yang, Q. Su, W. Lan, E. Xie, Lightweight, interconnected VO2 nanoflowers hydrothermally grown on 3D graphene networks for wide-voltage-window supercapacitors, RSC Adv. 7 (2017) 35558–35564.

[118] M. Gholinejad, M. Bahrami, C. Nájera, A fluorescence active catalyst support comprising carbon quantum dots and magnesium oxide doping for stabilization of palladium nanoparticles: Application as a recoverable catalyst for Suzuki reaction in water, Mol. Catal. 433 (2017) 12–19.

[119] S. Yuan, J. Gu, Y. Zheng, W. Jiang, B. Liang, S.O. Pehkonen, Purification of phenol-contaminated water by adsorption with quaternized poly (dimethylaminopropyl methacrylamide)-grafted PVBC microspheres, J. Mater. Chem. A. 3 (2015) 4620–4636.

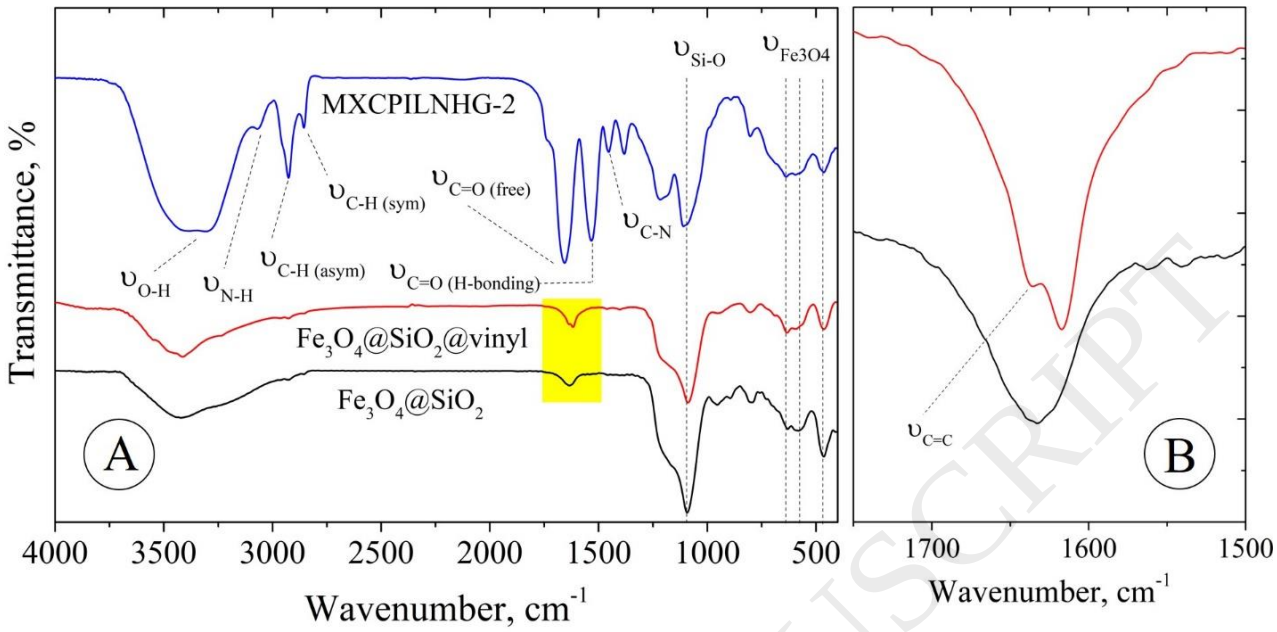

Figure 1. FT-IR spectrum of Fe_3O_4@SiO_2, Fe_3O_4@SiO_2@vinyl and MXCPILNHG-2 (A) and the extended FT-IR spectrum of Fe_3O_4@SiO_2 compared with Fe_3O_4@SiO_2@vinyl (B).

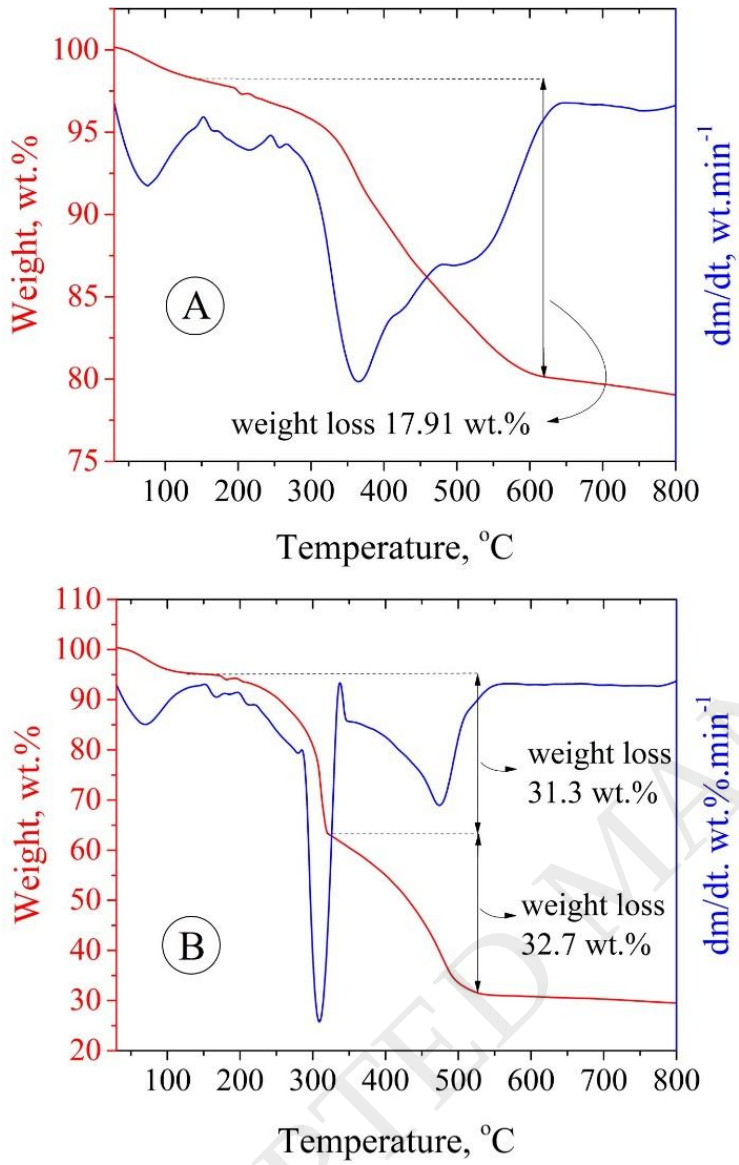

Figure 2. TGA and DTG thermograms of Fe_3O_4@SiO_2@vinyl (A) and MXCPILNHG-2 (B).

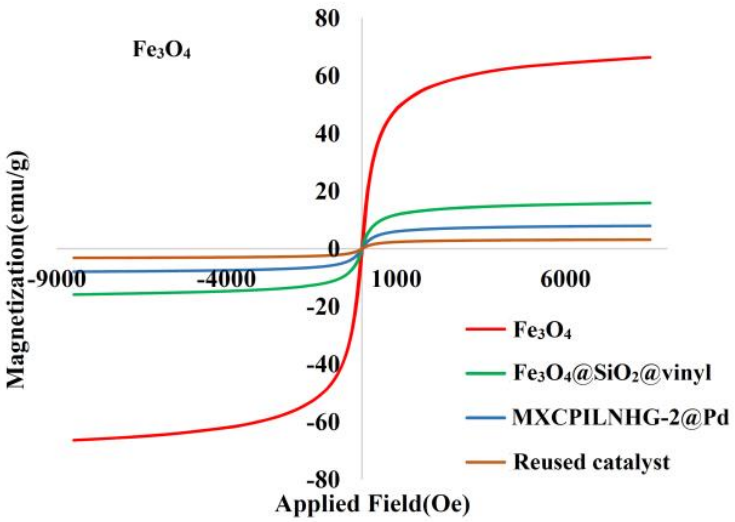

Figure 3. Magnetization curves for Fe_3O_4 NPs, Fe_3O_4NPs@SiO_2@vinyl, MXCPILNHG-2@Pd and reused MXCPILNHG-2@Pd.

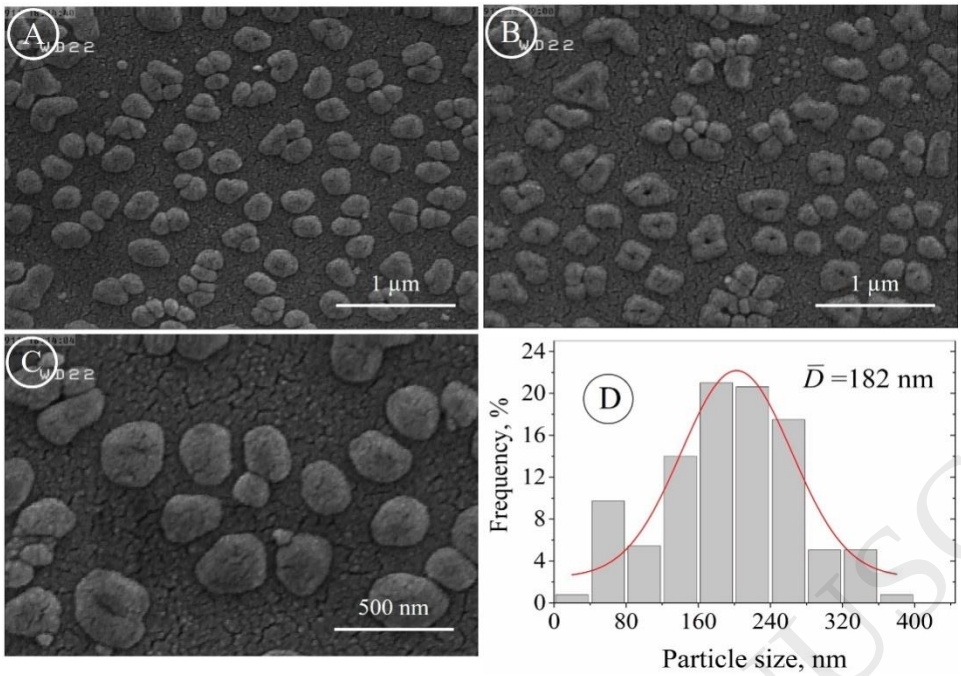

Figure 4. FE-SEM micrographs of MXCPILNHG-2 particles with paste-like morphology (A-C) and relatively narrow size distribution (D). Solid curve is Gaussian fit to the data.

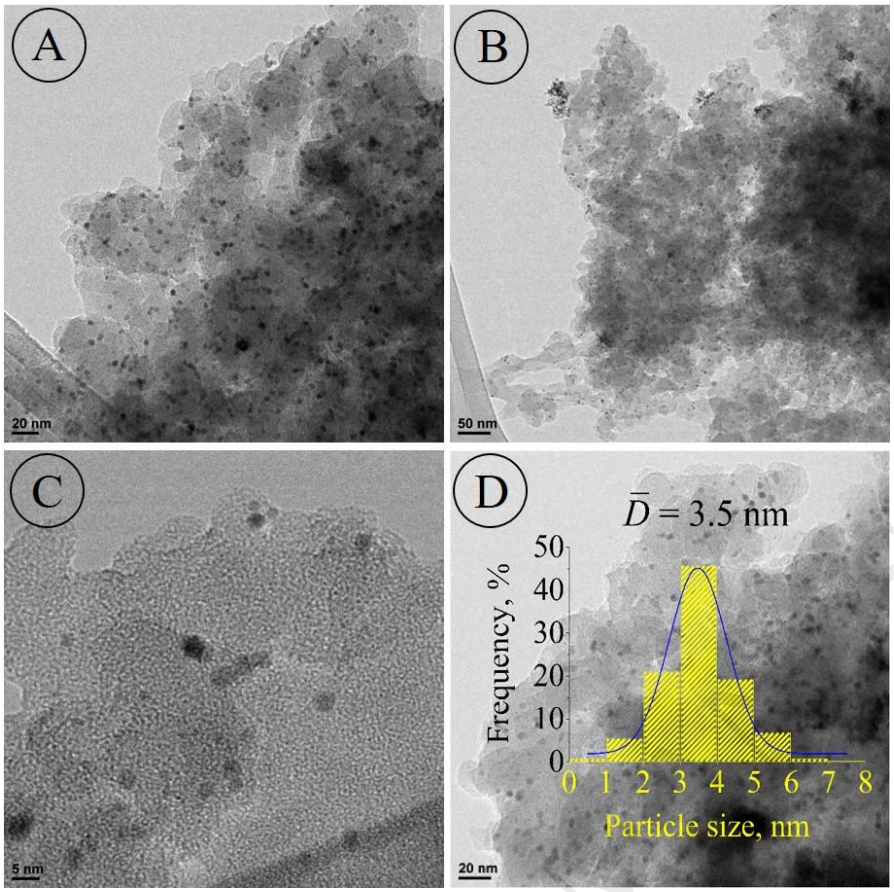

Figure 5. TEM images of MXCPILNHG-2@Pd in different magnification. The solid curve is Gaussian fit to the data.

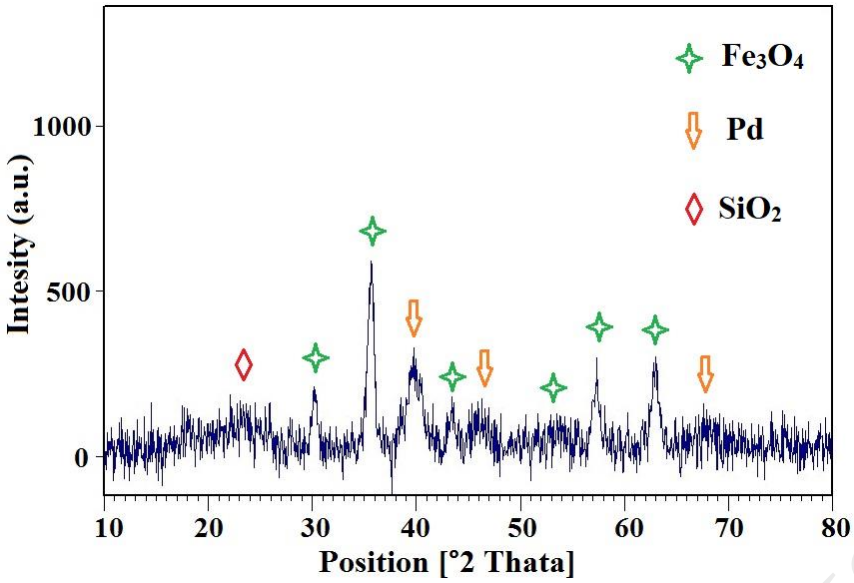

Figure 6. XRD pattern of MXCPILNHG-2@Pd.

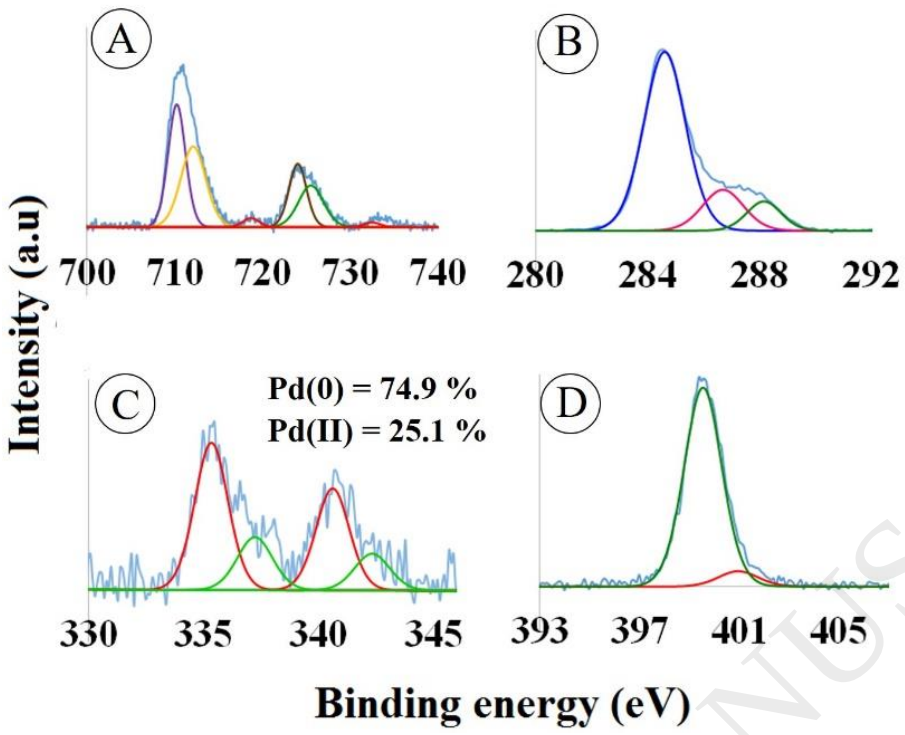

Figure 7. XPS spectrum of MXCPILNHG-2@Pd in A) Fe 2p, B) C 1s, C) Pd3d and D) N 1s regions.

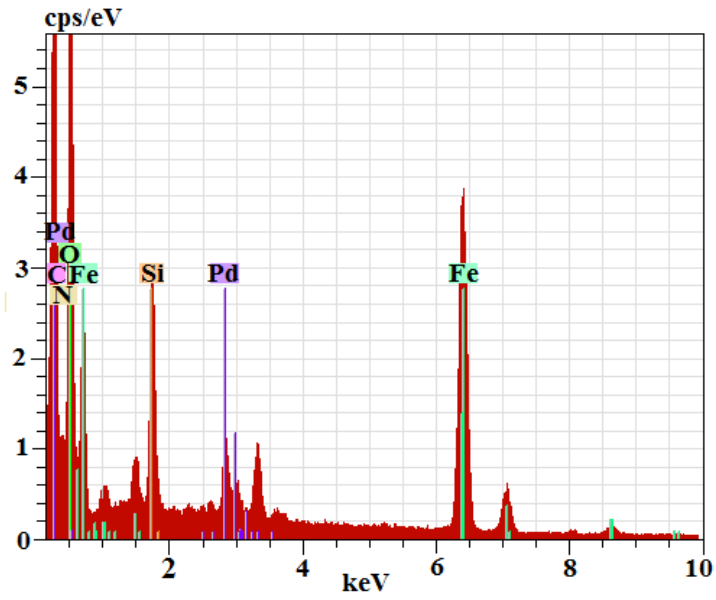

Figure 8. EDX spectrum of MXCPILNHG-2@Pd.

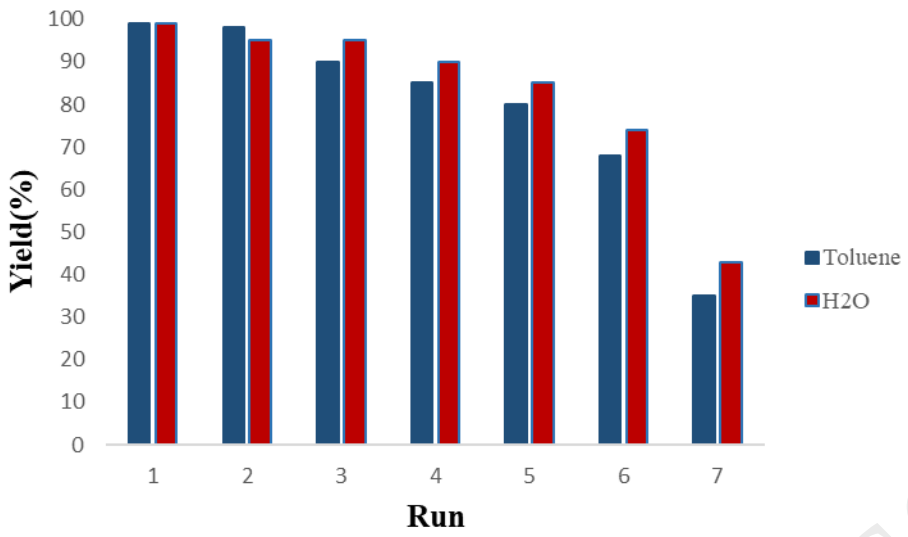

Figure 9. Recycling of the catalyst (MXCPILNHG-2@Pd) for the oxidation reaction of benzyl alcohol in toluene and H_2O.

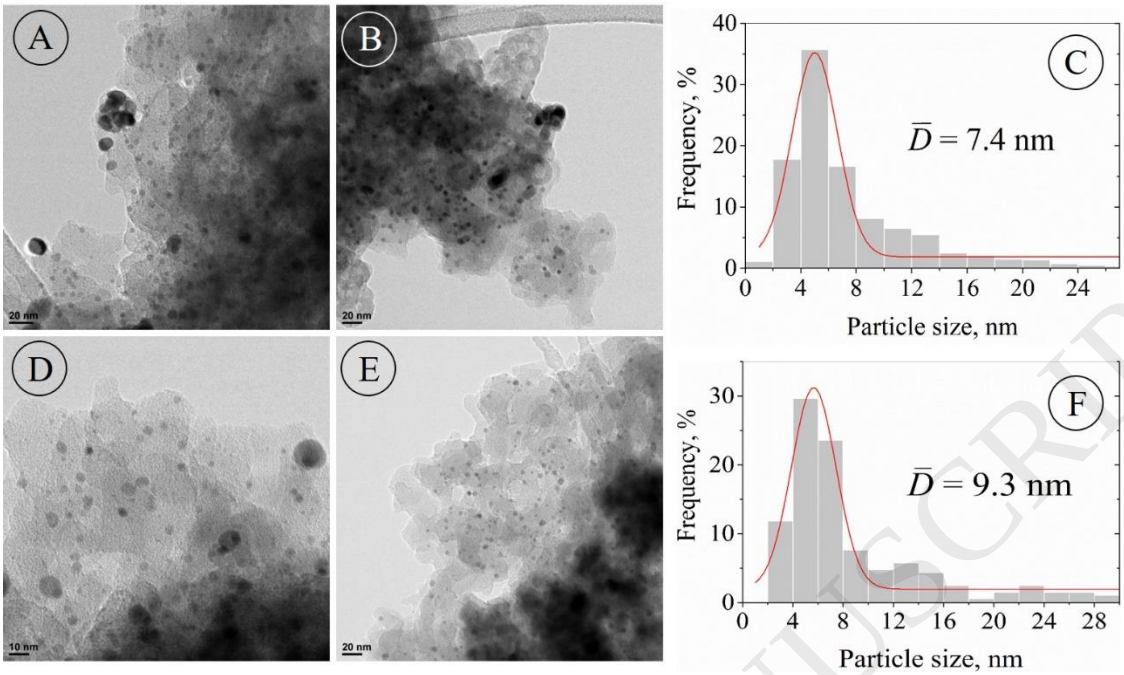

Figure 10. TEM images of reused catalyst (MXCPILNHG-2@Pd) after 5 runs in toluene (A-C) and H_2O (D-F).

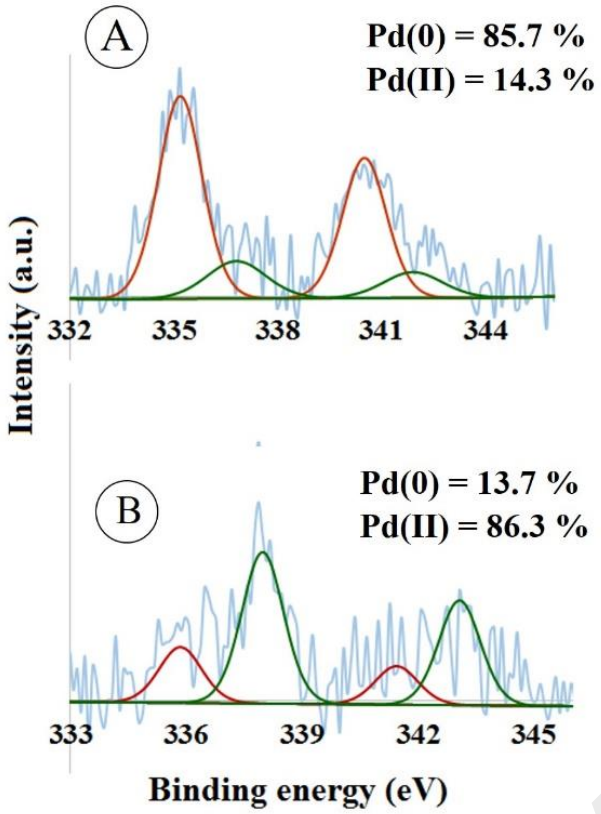

Figure 11. XPS spectrum of reused MXCPILNHG-2@Pd in Pd 3dregion for the oxidation reaction of benzyl alcohol; A) Toluene and B) H_2O.

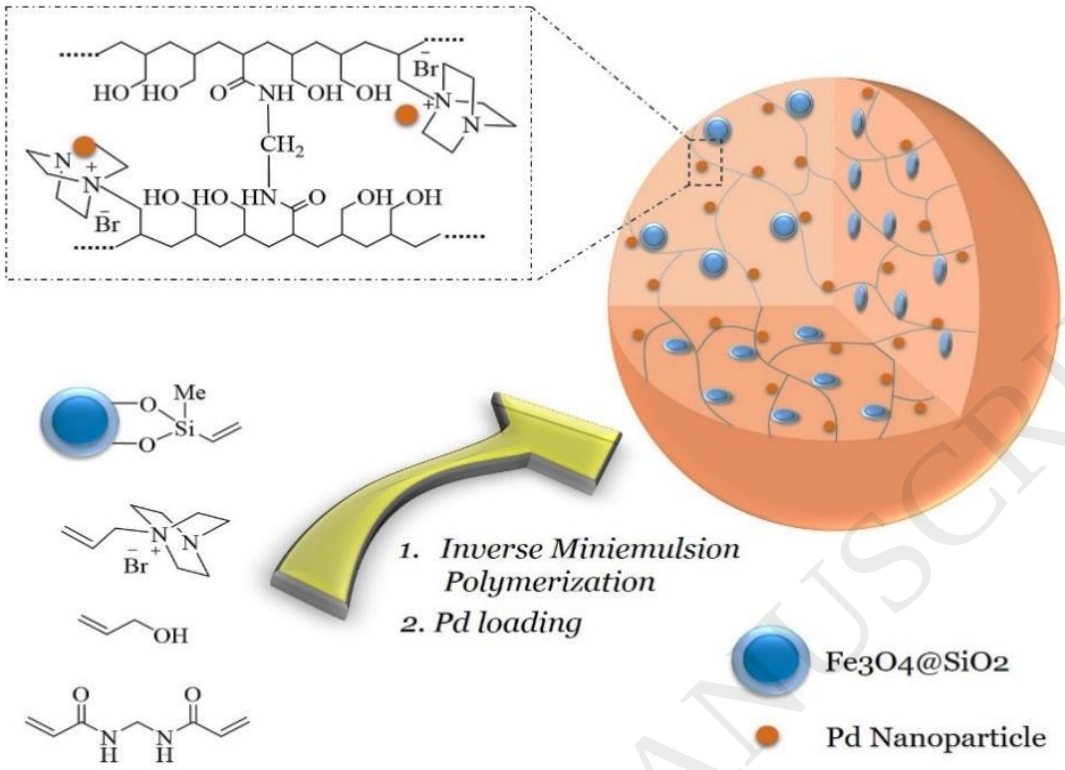

Scheme 1. Steps for preparation of MXCPILNHG@Pd NPs.

Table 1. Optimization of reaction condition for the oxidation of benzyl alcohol in the presence of MXCPILNHG-2@Pd[a]

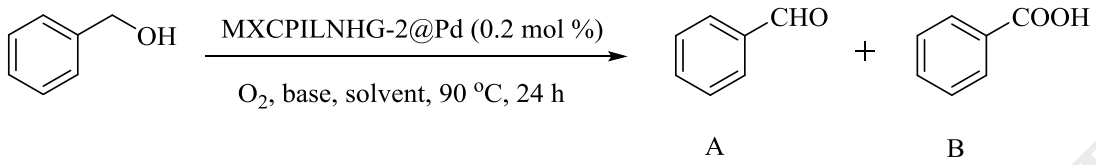

Entry	Solvent	Base	Conv. (%)[b]	A (%)	B (%)
1	1,4-Dioxane	K_2CO_3	5	5	----
2	CH_3CN	K_2CO_3	52	52	----
3	DMA	K_2CO_3	11	11	----
4	H_2O	$Na(OAc)_2$	15	10	5
5	H_2O	*t*-BuOK	35	25	10
6	H_2O	Free Base	15	4	11
7	Toluene	$Na(OAc)_2$	43	43	----
8	Toluene	*t*-BuOK	32	29	3
9	Toluene	Free Base	37	37	----
10	H_2O	K_2CO_3	28	10	18[c]
11	Toluene	K_2CO_3	38	38[c]	----
12	H_2O	K_2CO_3	50	5	35[d]

13	Toluene	K_2CO_3	88	88[d]	----
14	Toluene	K_2CO_3	67	67[e]	----
15	H_2O	K_2CO_3	93	6	87[e]
16	Toluene	K_2CO_3	2	2[f]	-
17	H_2O	K_2CO_3	4	2	2[f]

[a] Reaction conditions: benzyl alcohol (0.5 mmol), base (0.75 mmol), solvent (2 mL), catalyst (10 mg containing 0.2 mol % Pd).

[b] GC yields.

[c] Reactions using 0.1 mol % catalyst.

[d] Reactions performed during 12 h.

[e] Reactions performed at 75 °C.

[f.] Reactions using Fe_3O_4@SiO_2@Pd (average yield of the two reactions).

Table 2: Aerobic oxidation of structurally different primary alcohols in the presence of MXCPILNHG-2@Pd[a]

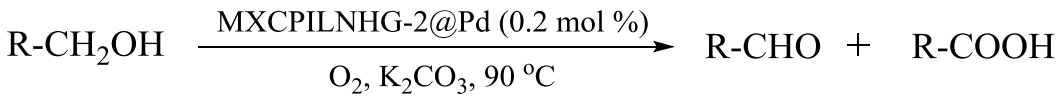

Entry	Alcohol	Solvent	Conv. (%)	Aldehyde (%)	Acid (%)	TON [TOF (h^{-1})]
1	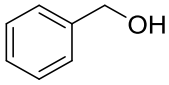	H_2O	>99	1	99	250 [10.4]
		Toluene	>99	98	2	250 [10.4]
2	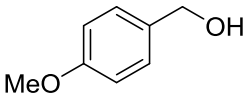	H_2O	96	5	91	240 [10]
		Toluene	93	93	-----	232 [9.6]
3	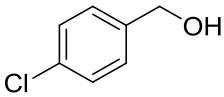	H_2O	99	19	80	247 [10.3]
		Toluene	80	80	-----	200 [8.3]
4	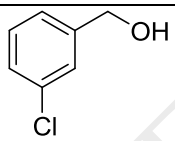	H_2O	>99	12	88	250 [10.4]
		Toluene	96	96	-----	240 [10]
5	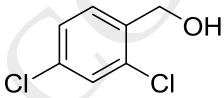	H_2O	62	10	52	155 [6.4]
		Toluene	88	88	-----	220 [9.1]
6	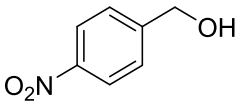	H_2O	>99	-----	>99	250 [10.4]
		Toluene	76	76	-----	190 [7.9]

7	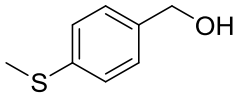	H_2O	99	83	16	247 [10.3]
		Toluene	90	90	-----	225 [9.3]
8	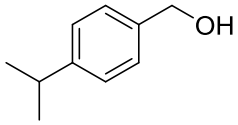	H_2O	>99	10	90	250 [10.4]
		Toluene	93	93	-----	232 [9.6]
9	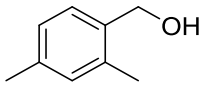	H_2O	99	3	96	247 [10.3]
		Toluene	>99	>99	-----	250 [10.4]
10	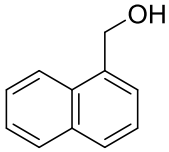	H_2O	75	75	-----	187 [7.8]
		Toluene	>99	>99	-----	250 [10.4]
11	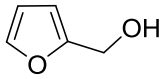	H_2O	-----	-----	-----	-----
		Toluene	96	96	-----	240 [10]
12	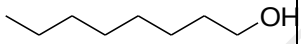	H_2O	>99	-----	>99	250 [10.4]
		Toluene	94	94	-----	235 [9.7]
13	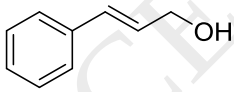	H_2O	62	60	2	155 [6.4]
		Toluene	91	91	-----	227 [9.4]

[a] Reaction conditions: alcohol (0.5 mmol), K_2CO_3 (0.75 mmol), solvent (2 mL), catalyst (10 mg containing 0.2 mol % Pd), and O_2 atmosphere.

Table 3: Aerobic oxidation of secondary alcohols in the presence of MXCPILNHG-2@Pd[a]

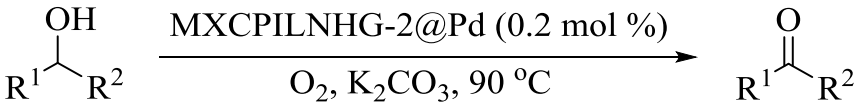

Entry	Alcohol	Solvent	Conv. (%)	Yield (%)	TON [TOF (h^{-1})]
1	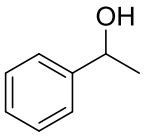	H_2O	90	90	225 [9.3]
		Toluene	98	98	245 [10.2]
2	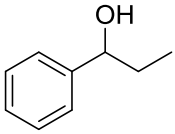	H_2O	>99	>99	250 [10.4]
		Toluene	>99	>99	250 [10.4]
3	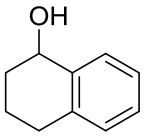	H_2O	>99	>99	250 [10.4]
		Toluene	>99	>99	250 [10.4]
4	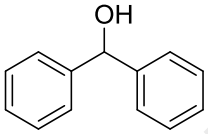	H_2O	89	89	222 [9.2]
		Toluene	>99	>99	250 [10.4]
5		H_2O	85	85	212 [8.8]
		Toluene	91	91	227 [9.4]
6	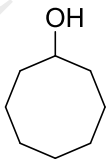	H_2O	88	88	220 [9.1]
		Toluene	25	25	62 [2.6]

[a] Reaction conditions: alcohol (0.5 mmol), K_2CO_3 (0.75 mmol), solvent (2 mL), catalyst (10 mg containing 0.2 mol % Pd), and O_2 atmosphere.

Table 4. Comparison catalytic activity of MXCPILNHG-2@Pd with other reported Pd catalysts in aerobic oxidation of benzyl alcohol

Catalyst	T (^{o}C)	Pd (mol %)	Conv. (%)	TON [TOF (h^{-1})]
Pd@PMO-IL [40]	95	0.25	>99	396 [132]
PdNP@poly-POSS-T_{mix} [41]	90	1.2	>99	41.25 [6.8]
PdNP@Extract [43]	80	2.5	95	38 [3.1]
Pd@MIL-88B-NH_2@SiO_2 [51]	150	2	98	49 [4.9]
Pd-pol [52]	100	0.5	75	150 [25]
SiO_2@APTES-Pd [53]	80	0.2	76	380 [15.8]
PdNPs/PS [56]	85	0.5	98	98 [6.5]
AmP-SNC/Pd(0) [58]	90	1	94	940 [940]
Fe_3O_4@SiO_2-2N-Pd(II) [62]	100	0.4	95	237 [29.6]
Fe_3O_4@CyS-Pd [63]	50	0.36	85	472 [314]
SiO_2@Fe_3O_4-Pro-Pd [67]	90	0.5	96	192 [19.2]
Fe_3O_4@ HPEI .Pd [68]	r.t	1	12	12 [12]
MNP-triazolyl- Pd$(OAc)_2$ [74]	90	1.9	90	23.7 [5.3]
MXCPILNHG-2@Pd	90	0.2	>99	250*5 [10.4]